

## Neuromorphic Engineering: In Memory of Misha Mahowald

**Carver Mead**

*carver@caltech.edu*

*California Institute of Technology, Pasadena, CA 91125, U.S.A.*

**We review the coevolution of hardware and software dedicated to neuromorphic systems. From modest beginnings, these disciplines have become central to the larger field of computation. In the process, their biological foundations become more relevant, and their realizations increasingly overlap. We identify opportunities for significant steps forward in both the near and more distant future.**

### 1 Introduction ---

Since before the dawn of computation devices, deep thinkers have mused on the capabilities of brains and whether there could be machines that could emulate some of their capabilities. With the advent of each new technology, it became the model of “the kind of thing that must be going on in the brain.” The brain must be like a clockwork, then a telegraph system, then a telephone system, then a digital computer, and now like the Internet. So the quest to make something that “works like the brain” has come to mean very different things to different people.

The first issue of *Neural Computation* in 1989 contained papers based on two seemingly totally unrelated views, leading to divergent threads of endeavor:

- The use of backpropagation in training multilayer neural networks, based on the ability of computer programs running on general-purpose computers to receive inputs and learn from them
- The creation of special-purpose, low-power silicon integrated circuits to analyze real-time sensory signals, based on the ability of living creatures to respond to their environment in “intelligent” ways

Fast-forward to 2022, when, ironically, Moore’s law has propelled the first thread onto the center stage of industrial computation, while the second has only recently seen commercial development. We will find that this divergence is illusory and that at a deeper level, the two threads are actually converging. We explore how this came about and what it might be telling us about the future.

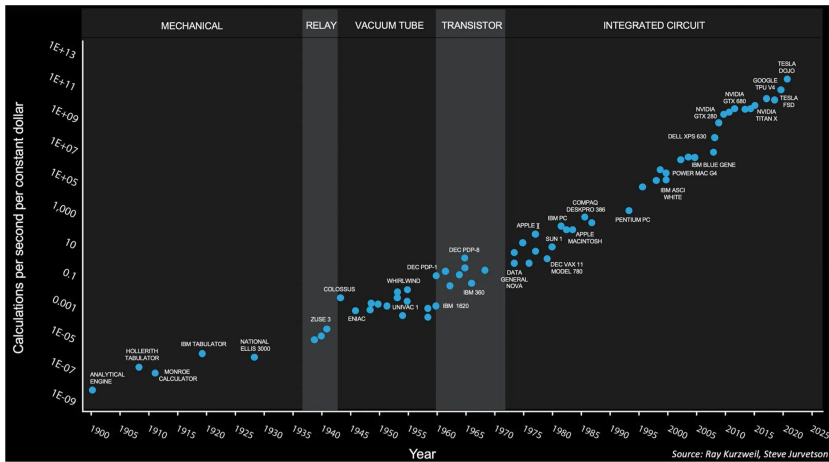


Figure 1: Real cost of computation versus year. (Graph: Steve Jurvetson, CC BY 2.0.)

## 2 General-Purpose Computing

In 1989, neural networks were assumed to be computer programs that ran on general-purpose computers. The evolution of general-purpose computing machines is well portrayed in Figure 1. Notice that computation is the number of operations per second: we can always get more operations by waiting longer.

How do we understand this remarkable evolution? Historically, over the long run, the cost of computation has been directly related to the energy used in that computation. Today's electronic wristwatch does far more computation than the Whirlwind did when it was built (Redmond & Smith, 1980). It is not just the computation itself that costs; it is the energy consumed and the system overhead required to supply that energy and get rid of the heat: the boxes, the connectors, the circuit boards, the power supply, the fans—all of the superstructure that makes the system work. As the technology has evolved, it has always moved, in fits and spurts, in the direction of lower energy per unit computation. That trend took us from mechanical gadgets to relays to vacuum tubes to transistors to integrated circuits. It was the force behind the transition from NMOS to CMOS technology that happened around 1980.<sup>1</sup> Today, it is still, by Moore's law, pushing us down to nanometer sizes in semiconductor technology.

<sup>1</sup>For that reason, this review concentrates on energy per computation as the central long-term theme. There are often other commercial considerations that dominate technology choices, but we will not dwell on them here.

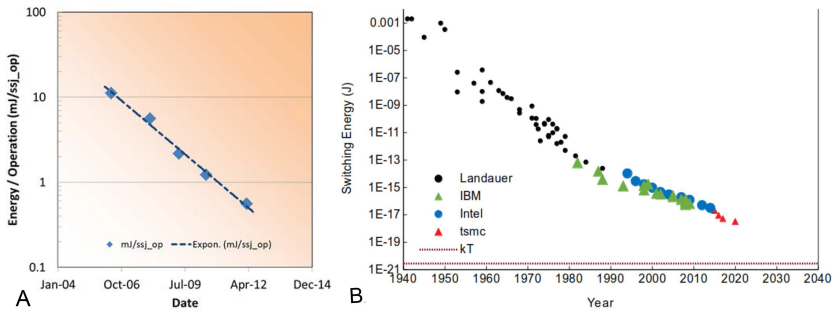


Figure 2: (A) Energy per operation at the server level (Saunders, 2012). (B) Energy to switch a single transistor (lesswrong.com). Both the square points in the left plot and the round blue points in the right plot represent Intel technology.

The energy dissipated in a digital switching event is  $\frac{1}{2}CV^2$ , where  $C$  is the capacitance and  $V$  is the signal voltage. As the individual elements of the integrated circuit (transistors and wires) have been made smaller over the years, the capacitance  $C$  of each electrical node has decreased and the power-supply voltage  $V$  has decreased accordingly. Thus, the energy required to charge an electrical node from a logic-0 to a logic-1 has decreased. As the transistors are made smaller, the length of the path an electron travels to move from one side of a transistor to the other gets shorter. The time required for a transistor logic circuit to switch is directly proportional to this “transit time.” As the dimensions shrink, the distance from one transistor to another decreases, the wire connecting them will thus be shorter, so it will take signals less time to get from one end to the other. The net result is that smaller feature sizes create computing circuits that run faster and use much less energy. That trend is shown in Figure 2. When we compare the two graphs for 2010, a server operation cost an energy of  $\approx 10^{-3}$  J, and switching a single transistor cost  $\approx 10^{-16}$  J. There is a factor of  $\approx 10^{13}$  between the energy to make a transistor work and that required to do an operation the way we do it in a digital computer.

There are two primary causes of energy dissipation in the general-purpose digital systems we built in 2010, and a similar one (but perhaps a bit better) in the systems we build today:

1. We lose a factor of more than 1000 because of the way we build digital hardware. Even on the same chip, very few signals are local—most of the energy is expended moving data around rather than using those data where they originate. The capacitance of the gate is only a very small fraction of capacitance of the wire that takes the signal from where it originates to where it is used, so we spend most of our energy charging up the the capacitance of the wires and not just the

transistor gates. Signals that go off the chip onto a circuit board cost at least another two orders of magnitude in time and three orders of magnitude in energy;

2. We use far more than one transistor to do an operation. “Today’s many-core processors have parallel single instruction multiple data (SIMD) instruction sets for floating-point, and dedicate around 1 million transistors per core to handling floating-point operations” (INRC, 2021).

The factor-of-1000 opportunity requires us to make algorithms more local, so that we do not have to ship the data all over the place. That is a big win: we have built digital chips that way and have achieved factors of 10 up to 1000 reduction in power dissipation for the same operation. Factors like that have gradually been making their way into the systems shown in Figure 1. Whenever there are operations that we want to do a lot of, they start bogging down the main computer—things like interfacing with the printer or the network, sound output, or the display screen—and some clever people figure out a way to make a special-purpose digital circuit that *just does that thing*. These application-specific integrated circuits can be tightly crafted to minimize wiring overhead and data movement, since they do not have to be “general purpose.” We will see a lot of this later.

By the year 1989 that we are commemorating, workstations and high-end PCs included built-in support for sound and quality color graphics. It was the games market that drove the development of quality computer graphics for many years, since interaction time is key for games. The demand for higher-quality graphics drove the development of increasingly sophisticated graphics processing units (GPUs), devices that end up playing a pivotal role in our story.

Also in 1989, the first commercial Internet service providers (ISPs) emerged in the United States and Australia, and what had been the ARPANET, along with a motley assortment of small and large private networks, were merged to become the Internet. To provide high-bandwidth interconnection over long distances required the development of an entirely new technology, and a relatively new field of endeavor, quantum optics, took center stage. Optical fibers with unimaginably low loss were developed, along with new kinds of semiconductor lasers, modulators, wavelength-division multiplexors—and the list goes on. Residual attenuation in fibers is compensated by ingenious in-fiber amplification, enabling a single fiber to transmit many optical channels, each channel carrying hundreds of gigabits per second, over spans of thousands of kilometers.

Also in 1989, Sequoia Data Corp. introduced Compumarket, the first Internet-based system for e-commerce. Sellers could post items for sale, and buyers could search the database and make purchases with a credit card. From this modest beginning, the Internet has emerged as host for an entire digital economy that has become a substantial fraction of the entire world

economy. In addition to sellers of traditional goods and services, the Internet makes possible entirely new kinds of enterprises that offer entirely new information-based products and services. Successful enterprises in the digital economy have grown to become some of the most highly valued companies in the world. Because the value created by many of these firms is based on information rather than on physical goods, they have developed huge data centers to house large clusters of computation and data-storage servers, the term *server* indicating “accessible from the Internet.” Thus “the cloud” came to be populated with enormous computing resources and even more enormous troves of organized data.

The wide availability of computers equipped with GPUs led those with applications that required heavy specialized processing to adapt their algorithms to run on GPUs. For anything that was a bit different from standard graphics processing, those adaptations were always a challenge.

### 3 Neural Networks

---

The neural network community arose from several disparate sources:

- Computer scientists, disappointed by the many high-profile failures in traditional artificial intelligence (AI) and believing that neurobiology provided clues that might enable a way forward
- Neurobiologists, who believed that computer simulation might provide a path to better understand their neural observations
- Engineers and physicists, who believed that the brains of animals worked on principles vastly different from those in known computers and that discovering these principles was the key to an entire new computing paradigm
- Theorists who believed that the key to understanding was through mathematical analysis

The field became popular immediately in academic circles. With the introduction of the backpropagation algorithm for minimization of error (Rumelhart, Hinton, & Williams, 1986; Durbin & Rumelhart, 1989) as an effective way to train multilayer networks, slow but steady progress was being made on problems of interest in the real world. So until 2012, this largely academic discipline was chugging along, with occasional spinoffs into the commercial sector. Then, in 2012, all that changed.

**3.1 The Tipping Point.** Alex Krizhevsky (2021), a young Ukrainian immigrant living in Canada, was good at coding—so maybe he should just get a job doing that—it paid good money. Then he stumbled on a story about machine learning and found a group at the University of Toronto that specialized in just that. Alex was admitted to the university’s PhD program, with Geoffrey Hinton as his adviser. Hinton had invented a class of networks called *restricted Boltzmann machines* and was pursuing their

application to image recognition, so Alex joined the effort. By 2009, he had finished his MSc thesis, “Learning Multiple Layers of Features from Tiny Images” (Krizhevsky & Hinton, 2009). In the process, he and his fellow graduate student Vinod Nair had developed two important data sets: CIFAR-10 and CIFAR-100 (Canadian Institute for Advanced Research, 10 and 100 classes)—both labeled subsets of the 1.6 million “tiny images” data set.

Both Alex and Nair continued working on image-recognition problems. Nair was still working with restricted Boltzmann machines in 2010 when he discovered that using a rectified linear unit (ReLU) nonlinearity in place of the almost universal tanh improved their learning performance (Nair & Hinton, 2010). It has turned out that the ReLU, which resembles activation curves found in many biological systems much more closely than a tanh does, has a number of advantages in deep neural networks and now is nearly universally adopted.

Alex experimented with modified versions of the ReLU in a number of convolutional deep belief networks (which contained restricted Boltzmann machines). He trained them on the tiny-images data set and tested the trained networks on the CIFAR-10 test set. His best network achieved a 78.9% accuracy, roundly beating the previous record of 74.5% (Krizhevsky & Hinton, 2010). In his paper, he comments, “The most computationally-intensive networks that we describe here take 45 hours to pre-train and 36 hours to fine-tune on an Nvidia GTX 280 GPU. By far, most of the time is spent squeezing the last few fractions of a percent from the nets.”

Alex and his adviser took different lessons from this result. Hinton concluded that “current methods for recognizing objects in images perform poorly and use methods that are intellectually unsatisfying . . . artificial neural networks should use local ‘capsules’ that perform some quite complicated internal computations on their inputs and then encapsulate the results of these computations into a small vector of highly-informative outputs” (Hinton, Krizhevsky, & Wang, 2011). So he put Alex on a project to learn how to train input layers of networks to learn such “capsules,” thinking that there might be a respectable PhD thesis in it for Alex.

But Alex had blood in his teeth: he had seriously beaten the tiny-images record, and his paper on that accomplishment had not even been published! And that accomplishment had not required anything “intellectually satisfying.” What he needed was more powerful GPUs and to squeeze every possible operation out of them.

From his work with various-sized networks and data sets of various-sized images, he had developed a “gut feeling” that training a network with many more layers and therefore many more weights was possible by very clever use of the detailed capabilities of the GPUs. He set out to create a computing environment based on a graphics system with two of the new, state-of-the-art GTX 580 3GB GPUs—with many long nights in the bowels of the GPUs, painfully finding every possible connection and its exact

timing. Then the fog cleared: he found a mapping of a multilevel network onto the GPUs that used all their capability maximally effectively!

In 2011, Alex's fellow gradate student Ilya Sutskever found out about the ImageNet LSVRC contest to classify 1.2 million high-resolution images into 1000 different classes. This is the event where, each year, the heavyweights in neural network technology compete to create and train their network on a really hard problem. The prize goes to the network with the lowest error rate in solving that problem. Ilya thought that Alex's experience in crafting neural network architectures and his mastery of the new GPUs might be up to the challenge, so the two decided to go for it.

The role of "intellectually satisfying" reasoning started on page 1 of their paper describing the results:

To learn about thousands of objects from millions of images, we need a model with a large learning capacity. However, the immense complexity of the object recognition task means that this problem cannot be specified even by a dataset as large as ImageNet, so our model should also have lots of prior knowledge to compensate for all the data we don't have. Convolutional neural networks (CNNs) constitute one such class of models, . . . Despite the attractive qualities of CNNs, and despite the relative efficiency of their local architecture, they have still been prohibitively expensive to apply in large scale to high-resolution images. Luckily, current GPUs, paired with a highly-optimized implementation of 2D convolution, are powerful enough to facilitate the training of interestingly-large CNNs, and recent datasets such as ImageNet contain enough labeled examples to train such models without severe overfitting (Krizhevsky, Sutskever, & Hinton, 2017).

*Overfitting* is the term neural network people use for the tendency of networks to "memorize" all the examples in the training set but not "generalize"—recognize examples that were not in the training set. Their paper has an entire section—"Reducing Overfitting"—from which we learn that

the easiest and most common method to reduce overfitting on image data is to artificially enlarge the dataset using label-preserving transformations. . . . We employ two distinct forms of data augmentation, both of which allow transformed images to be produced from the original images with very little computation. . . . The first form of data augmentation consists of generating image translations and horizontal reflections. . . . This increases the size of our training set by a factor of 2048. . . . The second form of data augmentation consists of altering the intensities of the RGB channels in training images. . . . This scheme approximately captures an important property of natural images, namely, that object identity is invariant to changes in the intensity and color of the illumination.

These data set augmentation techniques are known as "hints" and were formally introduced by Abu-Mostafa in the cover paper of the July 1995

issue of *Neural Computation* (Abu-Mostafa, 1995). Even with these “hint” enlargements, Alex’s network still exhibited substantial overfitting. The section continues:

The recently-introduced technique, called “dropout” (Hinton, Srivastava, Krizhevsky, Sutskever, & Salakhutdinov, 2012) . . . consists of setting to zero the output of each hidden neuron with probability 0.5. The neurons which are “dropped out” in this way do not contribute to the forward pass and do not participate in backpropagation. So every time an input is presented, the neural network samples a different architecture, but all these architectures share weights. . . . We use dropout in the first two fully-connected layers. . . . Without dropout, our network exhibits substantial overfitting. Dropout roughly doubles the number of iterations required to converge.

So what was required to get good classification performance and still keep the network from overfitting was a combination of “intellectually satisfying” techniques and a “big hack attack”—trying a lot of variations of network architecture, guided by Alex’s increasingly keen intuition for *what actually worked*—*It was a really hard year!* It took six days to train a network on all those images and would have taken weeks or months without Alex’s “highly-optimized GPU implementation of 2D convolution and all the other operations inherent in training convolutional neural networks.” It took six months for these experiments to get to the same performance as published results for the 2010 competition. Hinton had been skeptical but could see that this work was going to become valuable, so he organized DNNresearch (Lardinois, 2013), with Alex, Ilya, and himself as owners.

The networks were getting better. By June 2012, when the training and validation data for the ILSVRC 2012 were released, Alex’s single network was regularly producing less than 20% error rate on the 2010 data set—soundly beating the best published value of 25.7%. Nonetheless, others were making progress, and the submission was not due until mid-September. The whole trio was now fully engaged in the effort—this is a *huge opportunity!* They found that the network could be improved by “pretraining” with the entire 2011 ImageNet Fall release—tune, tweak . . . September—deadline extended to September 30—tune, tweak—they submitted two entries:

1. The average of five networks: Trained only on the training data supplied for this 2012 contest
2. The above average: Further averaged with two networks trained on the entire fall 2011 release

Get some sleep! Hold your breath! Think about something else . . .

On October 8, preliminary error rates released to participants—*WOW!* Alex: 15.3% Next best: 26.2% They had *blown it away!* The official release



of the full results was not for another five days, but the word traveled like wildfire!

Alex capsuled his own deep belief: “Our results show that a large, deep convolutional neural network is capable of achieving record-breaking results on a highly-challenging dataset using purely supervised learning. . . . All of our experiments suggest that our results can be improved simply by waiting for faster GPUs and bigger datasets to become available.”

Yann LeCun, creator of convolutional neural networks, is quoted as saying, “This is proof—AlexNet is an unequivocal turning point in the history of computer vision!”

Thus, with “AlexNet,” the “New AI” was born: the key to the future was scale—more data, more computing cycles.

Google had started the Google Brain project in 2011 to use its huge GPU infrastructure to implement a truly enormous distributed deep-learning system, originally called DistBelief. Google had been supporting DNNresearch, and, a few months after the ILSVRC 2012 results were released, Google acquired DNNresearch. Clusters of GPUs became widely available as part of cloud computing, with more and more sophisticated methods developed for mapping the operations involved in deep learning onto the things that GPUs did the best. The size of networks that could be trained grew by orders of magnitude.

Success emboldened researchers to try approaches that appeared to be “brute force,” “wasteful,” “impractical,” or even “stupid,” such as using individual pixel values as direct inputs to the first layer of a deep network. Success in one application area encouraged bolder approaches in other areas—“If more is better, go for it!” The result is evident in Figure 3.

The Google team created many highly successful deep-neural-network-based products, among them the speech-recognition system that is used as a front end to Search, and TensorFlow—an open-source software library that allows anyone to use machine learning by providing the tools to train their own neural network. To supplement free access to TensorFlow, Google has made a lot of free time on its GPU clusters available to researchers developing and training their own networks. A huge number of innovations in network concept, application, and architecture ensued, contributed by rank amateurs and old-timers alike. Hinton’s capsules for example, came back in full force in ResNets, and on it goes.

As can be seen in Figure 3, as a result of success on the part of many developers, even the latest GPUs, when fielded in clusters in large data centers, threatened to require resources beyond those available.

But for every deep neural network that gets trained, many copies of the net with fixed weights are parceled out for users to simply use by applying their own inputs and evaluating the corresponding outputs. This phase of a network’s life, called *inference*, is vastly simpler than training the net, but many more people are doing it.

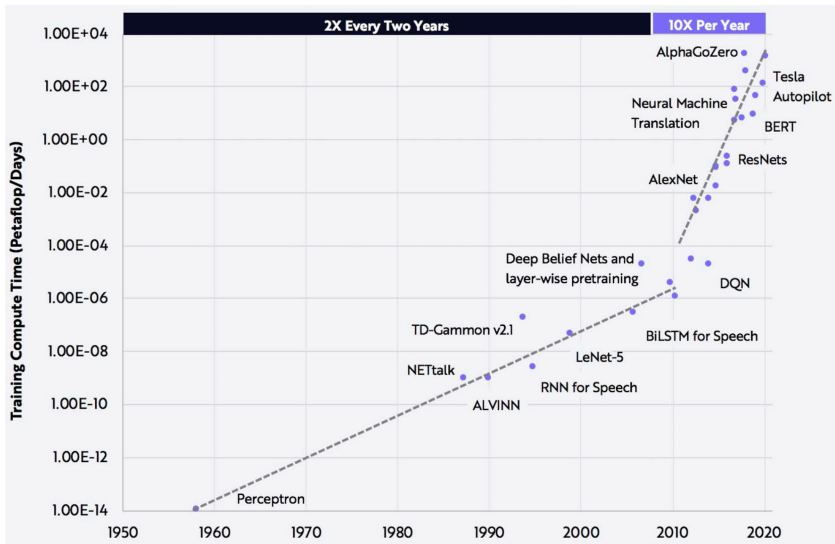


Figure 3: AlexNet starts a tidal wave! (OpenAI, <https://arxiv.org/abs/1603.04467>.)

To address what looked like a looming disaster from a large number of potential users, in 2013 Google launched a project to design a custom silicon chip, highly optimized for the operations most used in the application of neural nets. The project was under wraps until 2017 when an excellent paper appeared describing the chip, its history, and its performance (Jouppi et al., 2017).

By 2015, Norm Jouppi and his team had developed and fielded in its data centers a custom accelerator chip, the tensor processing unit (TPU). For neural network inference applications—evaluation of inputs on an already-trained network—they claimed 30 to 80 times more operations per watt-second than Intel CPUs and Nvidia GPUs of the same technology generation. Norm Jouppi, lead author on the Google announcement, explained how the project had come about: “The need for TPUs really emerged about six years ago, when we started using computationally-expensive deep learning models in more and more places throughout our products. The computational expense of using these models had us worried. If we considered a scenario where people use Google voice search for just three minutes a day and we ran deep neural nets for our speech recognition system on the processing units we were using, we would have had to double the number of Google data centers!” (Jouppi et al., 2017).

In 2017, when that statement was written, Google’s data centers used  $\approx 10^{13}$  watt-hours per year, thus running an average power of  $\approx 10^9$  watts. Google had  $\approx 10^9$  active users, so a single user accounted for an average of

just about 1 watt continuous. Three minutes' worth is  $\approx 1/500$  of a day, so to double the power usage per user, Google voice search on deep neural nets would be using 500 times the average power per user  $\approx 500$  watts, just doing inference, while it was being used.

The TPU chip used the group's knowledge of the flow of data in the execution of the neural inference algorithm to arrange the multiply/accumulate units physically next to each other so the data only need to move to the nearest neighboring units in the order that the operations are executed, as Jouppi describes:

The matrix unit uses systolic execution<sup>2</sup> to save energy by reducing reads and writes of the Unified Buffer. Data flows in from the left, and the weights are loaded from the top. A given 256-element multiply-accumulate operation moves through the matrix as a diagonal wavefront. The weights are preloaded, and take effect with the advancing wave alongside the first data of a new block. Control and data are pipelined to give the illusion that the 256 inputs are read at once, and that they instantly update one location of each of 256 accumulators (Jouppi et al., 2017).

The TPU is a beautiful example of minimizing data movement and interspersing memory with processing.

So even with gigawatts of power used by data centers, the execution of deep neural networks has required two steps of specialized silicon circuit design—the first for GPUs and the second for TPUs—in order to bring the power usage within reason. What started as a pure software endeavor is ending as an ever-increasing specialization of silicon circuits for performing neural operations.

More recently, what used to be GPUs aimed at speeding up graphics have increasingly morphed into dedicated deep-learning “accelerators.” Nvidia just announced the H100 (Andersch et al., 2022, named after Grace Hopper)—a huge chip (more than 8 cm<sup>2</sup>), with nearly half of its dense-processing area devoted to tensor operations. When fully running, the chip dissipates 700 watts. Cerebras (2022) has taken an even more audacious approach and made a wafer-scale system. Both companies realized that most of the time and power consumption goes into moving data around. And signals that need to go off the chip are by far the worst. The hardest part of going to a very large chip (like Nvidia) or wafer scale (like Cerebras) is dealing with the “bad spots” on the wafer; normal semiconductor practice is to just throw away the chips that have bad spots. But it is a universal experience in multilayer networks that weights and data in networks are inherently sparse, so if a value is zero, you don't need to send it. That idea generalizes to. Both companies use this technique to obtain good silicon use in spite

---

<sup>2</sup>The term *systolic* was introduced by Kung (1979, 1982), and Kung and Leiserson (1979).

of unavoidable defects. To take full advantage of sparsity, Intel's Loihi system (INRC, 2021), SpiNNaker (Hoppner et al., 2021), Cerebras's wafer-scale system (2022), and others use a message-based, event-driven interconnect protocol (more on this important topic later). For example, a multiply is not triggered until both operands are received. The Cerebras wafer-scale "chip" is 215 mm on a side. When fully running, it dissipates 20 kW, so it is water-cooled, but fits in a compact cabinet. It is claimed to do the work of an entire data center cluster, so having a personal version like this reminds us of the days when a computer required an entire air-conditioned room in a computing center and was accessed by time-sharing. And then minicomputers came along.

#### 4 Inference with Continuous Variables

---

As described above, inference in an  $n$ -deep network is basically  $n$  layer operations. Let's look at a layer that has  $i$  inputs and must compute  $j$  outputs, which become inputs for the following layer. That layer operation computes each output  $Q_j$  by multiplying each input  $V_i$  by a weight  $W_{ij}$ , adding the result to the total for that output and applying a nonlinear operation  $f(Q)$  to the sum, which becomes one input  $V_j$  to the next level:

$$Q_j = \sum_i W_{ij} V_i \quad V_j(\text{Level } n + 1) = f(Q_j)(\text{Level } n). \quad (4.1)$$

The values of the variables in equation 4.1 are continuous, and the weights are arrived at by a learning procedure (typically backpropagation) that incrementally adjusts the  $W_{ij}$  to minimize the error after each presentation or learning cycle. It is imagined that there is some error surface in weight space, and we wish to slide down to a minimum in that surface. Now a digital solution inherently quantizes the inputs, weights, and outputs to discrete values, so the error surface is no longer smooth but has steps all over it. So when we change the weights a bit, the output might not change, might change a little, or might change a lot, depending up whether it is close to the inevitable discontinuities or flat spots in the error surface due to discretization of the variables involved. For that reason, digital implementations of deep neural nets use a floating-point representation when they train the network by tweaking the weights. It is not that the absolute accuracy of the weights is necessarily high, since the weights are often truncated to short integers for the inference process (Dally et al., 2018), but it is an attempt to emulate a system that has a smooth derivative. So the first question we should ask is: Instead of faking, quasi-continuous variables with binary values, why not use continuous physical variables to start with? This experiment has only been done at small scale, so it remains for future innovators to determine if it is feasible for truly large deep neural nets.

**4.1 Inference in Analog Silicon.** Inference is the easy part; training is much harder. So let's see if there is a good way to do inference in a way that is more natural than Jouppi's TPU chip.

Electrically minded people realize immediately that if each weight is stored as a charge on the floating gate of an MOS transistor, the input is a voltage on the source of that transistor, and the drain current of that transistor (with the drain voltage held constant) will be some approximation to the product of the stored charge  $W_{ij}$  and the input voltage  $V_i$ . When that current is injected into a wire, shared with all  $i$  floating-gate transistors for the same output  $j$ , the resulting total current  $Q_j$  in the wire is the sum of the currents from all transistors connected to that wire (Kirchhoff would be happy):

$$Q_j \approx \int \sum_i W_{ij} V_i dt \quad V_j = f(Q_j). \quad (4.2)$$

There are many ingenious but simple transistor circuits that produce, smooth  $f(Q_j)$  nonlinearities (including smooth versions of the ReLU function discussed earlier) as a natural part of the current-to-voltage conversion that produces the input  $V_j$  to the next layer and clamps the wire voltage, so the array itself works in current-steering mode, thus dissipating very little energy. The interlayer circuits also implement a renormalization of the signal levels; they are the only part of the network that dissipates any significant power, which is thus order( $j$ ), not order( $j^2$ ).

In all the digital training experience over the years, it has been found that the form of the function  $f(Q)$  can make a substantial difference in the results obtained (Nair & Hinton, 2010). In analog circuits, quite sophisticated functions can be introduced that cost nothing in either energy or time. Such functions have a long history in the analog world; the ones that work reliably in practice are sufficiently rare that each is referred to by the inventor's name (e.g., the Gilbert multiplier).

In 1995, an appropriate technology for the inference task described above had an efficient small-scale proof of concept using such a floating-gate MOS technology, as shown on the left in Figure 4.

By 2011, a programmable analog array (Schlottmann & Hasler, 2011) using similar floating-gate synapse technology to store the weights could be field-programmed to do inference tasks with 1000 times less energy and 100 times less silicon area than the best digital solutions of the day. The current-mode differential synapse arrangement used is shown in Figure 4A. That arrangement can be programmed to produce two individual output currents or one differential output.

The  $i \times j$  array has these important properties:

- Each cell stores the weight  $W_{ij}$  in a nonvolatile manner.

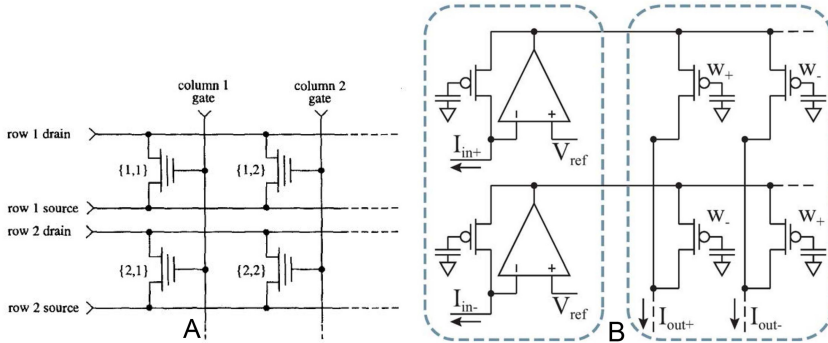


Figure 4: Floating-gate analog vector-matrix multiply arrays. (A: Diorio, Hasler, Minch, & Mead, 1996; B: Schlottmann & Hasler, 2011.)

- The cell multiplies the input by the stored weight to produce its contribution to the output current.
- The output wire, an integral part of the cell, sums the cell's output current with that of the other cells.
- The actual synapse circuit in the cell can (in a special process similar to EEPROM or Flash) be as small as a single transistor.

The widely acclaimed GPT-3 network has 175 billion weights connecting 8.3 million units arranged 384 layers deep ( $96 \times 3$ ) and 49,152 units wide. To compare a digital hardware implementation with a partially analog one, we consider a 50,000-wide, 400-layer network, with each layer fully connected to the next—for round numbers— $10^{12}$  weights.

In the 16 nm digital implementation described by Dally et al. (2018), each  $\approx 4$  bit multiply costs  $\approx 10^{-14}$  J and the shift/add costs about the same, so just the multiply/shift/add for the entire network would cost  $\approx 2 \times 10^{-2}$  J per inference step. But just feeding the digital weights to the processing unit on the same chip takes  $\approx 10^{-12}$  J per weight, which is  $\approx 100\times$  the energy cost of the local multiply/add operations. If the architecture allows the weights to be reused without moving them, the data-movement energy cost is reduced by the reuse factor, which Dally et al. (2018) give as 32. The weight movement plus multiply/add energy then comes to  $\approx .05$  J per presentation for a fully on-chip implementation. Used at a presentation rate of 30/sec this digital chip would dissipate 1.5 watts, and 10 to 100 times more power for weight storage on separate memory chips.

Let's estimate what that would look like in dedicated analog silicon. In a modern flash memory process, each synapse could be  $30 \text{ nm} = 3 \times 10^{-8} \text{ m}$  on a side (Goda, 2020). So each layer array with 50,000 inputs and 50,000 outputs could be  $\approx 1.5 \text{ mm}$  on a side. Since the outputs of one array go to the inputs of the next array, the entire network can be tiled into a

$20 \times 20$  array. When laid out in this way, the entire inference engine—400 layers each having 50,000 inputs and 50,000 outputs with all weights stored locally—would fit on a  $30 \text{ mm} \times 30 \text{ mm}$  chip—only slightly larger than the latest digital GPU/TPU chips, which require separate memory chips for weight storage—and pay the attendant energy and time penalty. The analog chip would execute  $10^{12}$  multiply/add operations per presentation and require  $2 \times 10^7$  interlayer functions. As in the digital implementation, the big energy drain will be the input interlayer circuits driving the input voltage  $V_i$  across the array. The total current addition on the array will require less energy, as the voltage across the weight transistors is less than the full signal voltage, and the total current is then supplied by the interlayer circuits. If we make the conservative assumption that each interlayer function costs the same energy as one of Dally's digital multiply/add plus one wire driven across the  $1.5 \text{ mm}$  width of the array, that would be  $\approx 10^{-13} \text{ J}$  per wire per presentation. For all  $400 \times 50,000$  interlayer circuits, the energy would come to a few  $\times 10^{-6} \text{ J}$  per presentation. At 30 presentations/sec the chip would dissipate  $\approx 10^{-4}$  watt. Pipelining between arrays, which can speed up throughput by substantial factors, can be accomplished in analog as it can in digital technology. By using this fully unrolled design, we have merged the memory and information processing, an approach that goes under the rubric of "in-memory computation" or "in-memory processing" and has recently received considerable attention (Sebastian, Le Gallo, Khaddam-Aljameh, & Eleftheriou, 2020; Liu, 2022; Mythic-ai.com, 2021; ISSCC, 2022).

There are several risks and costs associated with this analog approach:

1. The huge advantage of digital technology is that each signal is restored at each step of processing or storage. In contrast, traditional analog signals are not restored; signals propagating in any cascade of analog sections accumulate error and noise as they propagate, so any workable system must restore its signals after at most a few stages. In the above system, this restoration would logically take place in the current-sense circuits of at least every few network layers. Thus, a practical analog implementation will actually be a hybrid system— analog computation followed by "digital" restoration. All network designs do some version of restoration in the  $F(Q)$  interlayer function, but it will only become clear what effect the analog-necessitated restriction has on the overall capability of a many-level network by actually comparing one with and without these restrictions. Seems like a good PhD thesis project.
2. Moore's law has, over many process generations, optimized silicon fabrication processes for the densest digital circuits. The result has been that analog properties are, if not totally neglected, at least relegated to minor status. Reoptimizing a process for analog performance is a nontrivial undertaking.

3. As processes have scaled down in dimensions and supply voltage, the number of electrons representing a full-scale analog signal (or digital “one”) has decreased exponentially, yet it is still far from the true digital limit, where the presence or absence of a single electronic charge reliably represents a single digital bit. In this intermediate range of physical and electronic scales, inherent variations of properties from one transistor to another become a larger and larger proportion of a full-scale signal. Thus, the above approach increases the need for expert circuit design at the hardware level and clever resource allocation at the system level to work around individual-transistor variation (and chip defects, as discussed earlier).
4. Programming the chip for a specific network is an iterative process: each weight must be read, changed in the direction required, and then read again, and the cycle repeated until the desired weight is attained. This process requires a variable time for each weight on an expensive, dedicated programming facility;
5. Reprogramming after deployment requires the equivalent of the programming facility, which would require a level of power that may not be compatible with the overall low-power environment.

### The Bottom Line

1. An analog inference chip with resident weight storage can potentially achieve 10,000 times lower power and about the same silicon area as a single-chip self-contained digital implementation.
2. The analog chip would have different, and potentially more, restrictions than an efficient digital chip, with currently unknown consequences.
3. This programmable inference chip could be realized with a variant of today’s EEPROM or flash memory technology.
4. However, realizing the level of signal retention required for an analog representation could take a lot of development.
5. The effort might be worthwhile for applications where power consumption is paramount.

**4.2 Analog Backpropagation.** We saw that analog technology could be instrumental in reducing power in the evaluation (inference) phase, where the neural network is applied to a real problem by a real user, not the developer. It seems like the continuous nature of analog variables would be of even more value during the training phase of a deep neural network.

The following discussion is quite speculative. It would take a lot of effort—and some major inventions—to bring it about. We will encounter a number of alternatives to standard backpropagation in later sections, so this may not be the best way forward (see the caveats at the end of this section).



Let's look at how the array shown on the right in Figure 4 might be trained. For this discussion, we use the configuration where the output lines labeled  $I_{\text{out}+}$  and  $I_{\text{out}-}$  represent two separate outputs. One step in training each layer of the network with backpropagation consists of two passes through the network:

### Forward Pass

- Present input signals to the input  $i$  wires of the network.
- Inference: Propagate signals through weights in the forward direction as described for the inference chip.
- Compare the network  $j$  outputs with the desired outputs, thereby generating a vector of  $j$  error signals.

### Backward Pass

- Present the error signals to the  $j$  "output wires" of the network, now acting as inputs.
- Propagate these error signals backward through the same weights, thereby generating an error value on each of the  $i$  "input" wires to be fed back to the "previous" layer.
- Each "synapse" circuit uses its  $j$  error value to proportionally correct its own local weight.

Signal propagation on a wire and through a transistor can be quite symmetric. Since the same  $W_{ij}$  transistor is used on the forward and backward passes and its weight is adjusted by the learning process, transistor-to-transistor threshold variation is thereby reduced as a source of error. This arrangement also makes all the information necessary for backpropagation available locally to the weights to be updated.

In order to propagate signals in the reverse direction, the circuit implementing the nonlinear function  $f(V_i)$  at the (forward) output of each layer needs to be augmented with drivers for driving signals in the reverse direction and a mode control for selecting that pass the network is executing. Such circuits need to be done carefully. Transistor offset voltages in these interlayer circuits can potentially be reduced using the same floating-gate technology as is used in the synapse circuits. Pipelining between arrays, which can speed up the forward inference step by substantial factors, is not easily included in a fully unrolled backpropagation design.

The synapse circuit itself is even more challenging. The floating-gate learning rule described in Diorio et al. (1996) needs to use the local error signal on its  $j$  wire together with a global update command, presumably on a separate dedicated wire, to either increment or decrement the charge on the floating weight storage gate. An efficient solution to this design challenge would be a major contribution to the field. Optimal solutions require a fully integrated approach encompassing device physics, fabrication process, circuit design, system-level function, and layout.

For this discussion, I have concentrated on floating-gate storage technologies in a silicon technology for two reasons. First, I have personally worked with them, so I know more about them. Second, the processes by which they are fabricated are highly evolved, both technically and economically. It is possible to add and subtract charge from a floating gate in a nicely controlled way (Diorio et al., 1996). I am also aware that extensive progress is being made in other nonvolatile weight-memory technologies. Many of the above comments apply to them as well.

Since the weights must be stored somewhere, it is a huge win in both time and energy to store them where they are being trained. We can imagine (optimistically) that the learning-synapse circuit might be twice the size in each dimension of the inference synapse cell. So the entire deep network, with training and inference capability, can possibly be implemented in a chip four times the area of the inference-only chip, making it 60 mm × 60 mm—large but not impossible using the wafer-scale techniques discussed earlier. There are many ways to make such a chip relatively immune to bad spots, the simplest being just not allocating any of the bad rows or columns. This is, in some way, the analog counterpart to the Cerebras learning system.

All the caveats described for the inference chip apply, with even more weight, to this learning system. In addition, neither chip design has a mechanism for taking into account the observed sparsity of both weights and activations in this class of networks. Progress in the field at present is rapid, and digital implementations are evolving ever more clever methods for exploiting sparsity (Delbruck & Liu, 2019; Sommer, Özkan, Keszocze, & Teich, 2022). The brute-force analog implementations described above are useful in comparing energy efficiency of digital versus analog technologies but should not be taken as a preferred way forward.

A recent review (Parisi, Kemker, Part, Kanan, & Wermter, 2019) details one of the most severe limitations of backpropagation-style deep-learning networks:

Humans and animals have the ability to continually acquire, fine-tune, and transfer knowledge and skills throughout their lifespan. This ability, referred to as lifelong learning, is mediated by a rich set of neurocognitive mechanisms that together contribute to the development and specialization of our sensorimotor skills as well as to long-term memory consolidation and retrieval. Consequently, lifelong learning capabilities are crucial for computational learning systems and autonomous agents interacting in the real world and processing continuous streams of information. However, lifelong learning remains a long-standing challenge for machine learning and neural network models since the continual acquisition of incrementally-available information from non-stationary data distributions generally leads to catastrophic forgetting or interference. This limitation represents a major drawback for state-of-the-art deep neural network models that typically learn representations from

stationary batches of training data, thus without accounting for situations in which information becomes incrementally available over time.

For inspiration on real-time lifelong learning, we must look deeper into the most astounding example of energy efficiency, using fully integrated analog/digital elements: the human brain.

## 5 Sensory Neural Silicon

---

Since the human brain, using under 20 watts, is so good at many of the tasks that require so much power when done digitally, even though electronic devices are many orders of magnitude faster than neural ones, there have been efforts for many years to understand how brains do it with such inefficient components.

The second thread represented in the first issue of *Neural Computation* described simple analog circuits that emulate the temporal processing of signals in the brain (Lazzaro & Mead, 1989). Early neuromorphic chips like these concentrated on real-time sensory input because it is the primary source of data on which animal brains operate and no source of such data in the form suitable for input to neural computation is otherwise available.

Two high-bandwidth channels into the brain are auditory and visual. Primary stimuli (light for the eye and sound pressure for the ear) are transduced into a sequence of nerve pulses on the optic nerve of the eye and the auditory nerve of the ear. The only optical or auditory data the brain has access to are these pulse sequences. To carry all necessary real-time sensory information in an energy-efficient manner, the encoding of sensory information in these sequences must be extremely sophisticated; it is only partially understood after many years of intense study. The transducers themselves—the retina of the eye and the cochlea of the ear—are objects of wonder: each incorporates a great deal of signal processing as an integral part of the transduction process. It is no exaggeration to view each of these transducers as an outpost of the brain itself, located with and integrated into the transduction process. Each is, in its own right, the object of a major subfield of neurobiology.

**5.1 Auditory Sensing and Processing.** We start with auditory processing, since issue 1 of *Neural Computation* opened with a review of neural networks for speech recognition (Lippmann, 1989) and a description of a low-power neuromorphic chip, implementing an analog model of a simple hearing function (Lazzaro & Mead, 1989).

Dick Lyon's book (2017) takes a unique and enlightened engineering view of the workings of the human hearing system. This system functions seamlessly over a factor of more than a million in sound pressure. Over the lower factor of a thousand or so, the total number of nerve spikes per second in the auditory nerve is almost constant. This fact already tells us

a lot about the encoding and decoding of sound information in the brain. Given the ability of humans to enjoy the intricacies of orchestral music, for example, even at a low sound level, it must be true that every nerve spike carries a lot of information. Since the system has no “clock” like most digital systems do, we can intuit that information must be encoded in the relative time of arrival of nerve spikes on different nerve fibers. That information is analog in time and digital in amplitude. Neurobiologists have looked in many brain areas of many animals; wherever they have looked carefully, they have found that information is encoded in the relative time of arrival of nerve spikes on different nerve fibers (Gollisch & Meister, 2008).

In mammals, the first level of processing done in the cochlea is to propagate the sound signal from the eardrum along a mechanical/fluidic transmission line, arranged to have a fast velocity of propagation at the input end, tapering to a much lower velocity of propagation toward the opposite end. The net result is that the structure has a best frequency for any given position along the line—high near the input and lower farther along. This finding led early investigators to believe it could be characterized as a bank of frequency filters, but findings that the auditory nervous system responds primarily to transients made that oversimplified conjecture untenable. Each individual stage of the line has amplifying elements, controlled by an elaborate gain-control system that acts at both short and longer timescales. This system not only amplifies low-level signals that would otherwise be inaudible, but compresses the signal amplitude into a smaller range, hence the near constancy of firing rate at low sound levels. This same gain-control system emphasizes transients in an advantageous way. Each stage of the cochlea contains detector elements that originate nerve pulses for the auditory nerve.

For a successful electronic hearing system, both analog and digital techniques are necessary to process sound signals from a microphone. Early models of the cochlea were cascades of very low-power analog sections, which gave a good intuitive idea of the information-processing power of the physiological cochlea (Watts, 1993), but the propagating auditory signal accumulated noise as it went along. Rahul Sarpeshkar (2010) gives extensive treatment of low-power circuits and their relation to biological systems.

Many recent auditory processing chips have developed clever hybrid analog and digital systems that minimize power and silicon area in both analog and digital domains. A recent auditory chip (Kim et al., 2022; Kim & Liu, 2022) offers a complete, self-contained, real-time keyword-spotting system fabricated in 65 nm CMOS (2005 vintage process), using analog-time and digital-value signals. The active circuitry occupies 2 mm<sup>2</sup> and uses 23  $\mu$ watt of power, supplied from a single small photocell and conditioned by an on-chip regulator, which takes up more than twice the area of the speech-processing circuitry. The 2015 Google speech recognizer using 500 watts (large vocabulary) and this minuscule micropower speech recognizer (12-word vocabulary) represent two extreme examples of specialized

silicon for speech recognition. Both approaches are being actively pursued, and both are evolving rapidly to higher capability and lower power.

**5.2 Visual Sensing and Processing.** I use examples from the evolution of silicon retinas to illustrate a number of physical principles that can be used to implement computation primitives. These examples also serve to introduce general principles of neural computation and to show how these principles can be applied to realize effective systems in analog electronic integrated-circuit technology.

In 1868, Ernst Mach (Ratliff, 1965) described the operation performed by the retina in the following terms:

The illumination of a retinal point will, in proportion to the difference between this illumination and the average of the illumination on neighboring points, appear brighter or darker, respectively, depending on whether the illumination of it is above or below the average. The weight of the retinal points in this average is to be thought of as rapidly decreasing with distance from the particular point considered.

For many years, biologists have assembled evidence about the detailed mechanism by which this computation is accomplished. The neural machinery that performs this first step in the chain of visual processing is located in the outer plexiform layer of the retina, just under the photoreceptors. The lateral spread of information in the outer plexiform layer is mediated by a two-dimensional network of cells coupled by resistive connections. The voltage at every point in the network represents a spatially weighted average of the photoreceptor inputs. The farther away an input is from a point in the network, the less weight it is given. The weighting function decreases in a generally exponential manner with distance.

Using this biological evidence as a guide, Mead and Mahowald (1984) and Mahowald and Mead (1988) reported a silicon model of the computation described by Mach. In the silicon retina, each node in the network is linked to its six neighbors with resistive elements (made from cleverly biased transistors) to form a hexagonal array, as shown in Figure 5.

A single bias circuit associated with each node controls the strength of the six associated resistive connections. Each photoreceptor is a phototransistor working against two diode-connected MOS transistors biased in subthreshold and thus having an exponential current-voltage relation. The output voltage at the emitter of the phototransistor is thus proportional to the log of the incident light intensity, making changes in voltage equal to changes in  $\log(\text{intensity}) = \log(\text{image contrast})$ , independent of absolute illumination. The receptor output drives the corresponding node of the resistive network through a transconductance amplifier—used to implement a unidirectional conductance—so the photoreceptor acts as a voltage source driving the network with an adjustable source conductance. The amplifier draws no

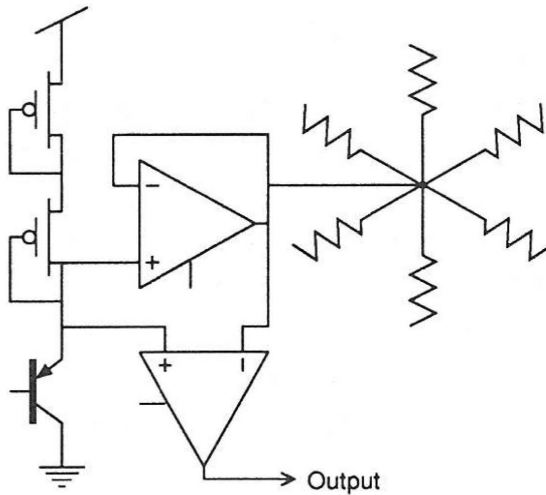


Figure 5: Earliest Mahowald retina pixel circuit. The output is the difference between the potential of the local receptor and that of the resistive network, which computes a weighted average over neighboring pixels (Mahowald, 1992).

current from the output node of the photoreceptor because its input is connected to only the gate of a transistor.

The resistive network computes a spatially weighted average of photoreceptor inputs. The spatial scale of the weighting function is determined by the product of the lateral resistance and the conductance coupling the photoreceptors into the network. Varying the conductance of the transconductance amplifier or the strength of the resistors changes the space constant of the network and thus changes the effective area over which signals are averaged. From an engineering point of view, the primary function of the computation performed by a silicon retina is to provide an automatic gain control that extends the useful operating range of the system. It is essential that a sensory system be sensitive to changes in its input, no matter what the viewing conditions. The structure executing this level-normalization operation performs many other functions as well, such as computing the contrast ratio and enhancing edges in the image. Thus, the mechanisms responsible for keeping the system operating over an enormous range of image intensity have important consequences with regard to the representation of data. We saw the same principle at work in the auditory system. It seems to be a universal theme in sensory systems, and we will see that it appears to have a central role at the highest level of brain function as well.

The image enhancement performed by the retina was also described by Mach (Ratliff, 1965):

Let us call the intensity of illumination  $u = f(x, y)$ . The brightness sensation  $v$  of the corresponding retinal point is given by  $v = u - m \left( \frac{d^2 u}{dx^2} + \frac{d^2 u}{dy^2} \right)$  where  $m$  is a constant. If the expression in parentheses is positive, then the sensation of brightness is reduced; in the opposite case, it is increased. Thus,  $v$  is influenced not only by  $u$  but also by its second differential quotients.

The image-enhancement property that Mach described is a result of not just one receptor but the receptive field of the retinal computation, which shows an antagonistic center-surround response. This behavior is a result of the interaction of the photoreceptors, the resistive network, and the output amplifier. A transconductance amplifier provides a conductance through which the resistive network is driven toward the photoreceptor potential. A second amplifier senses the voltage difference across that conductance and generates an output proportional to the difference between the photoreceptor potential and the network potential at that location. The output thus represents the difference between a center intensity and a weighted average of the intensities of surrounding points in the image. The center-surround computation sometimes is referred to as a Laplacian filter, which has been used widely in computer vision systems. This computation, which can be approximated by a difference in gaussians, has been used to help computers localize objects; this kind of enhancement is effective because discontinuities in intensity frequently correspond to object edges. Both of these mathematical forms express, in an analytically tractable way, the computation that occurs as a natural result of an efficient physical implementation of local normalization of the signal level. In addition to its role in gain control and spatial filtering, the retina sharpens the time response of the system as an intrinsic part of its analog computation. Effective temporal processing requires that the timescale of the computation be matched to the timescale of external events. The temporal response of the silicon retina depends on the properties of the horizontal network. The voltage stored on the capacitance of the resistive network is the temporally as well as spatially averaged output of the photoreceptors. Because the capacitance of the horizontal network is driven by a finite conductance, its response weights its input by an amount that decreases exponentially into the past. The time constant of integration is set by the bias voltages of the wide-range amplifier and the resistors. The time constant can be varied independent of the space constant, which depends on only the difference between these bias voltages rather than on their absolute magnitude. The output of the retinal computation is thus the difference between the immediate local intensity and the spatially and temporally smoothed image. It therefore enhances both the first temporal and second spatial derivatives of the image.

The original 1984 Mahowald retina gave us a realistic real-time model that shows essentially all of the perceptually interesting properties of early vision systems, including several well-known optical illusions such as

Mach bands. One problem with the first implementation of the circuit was its sensitivity to transistor offset voltages. Under uniform illumination, the output was not constant but contained a random fixed pattern reflecting the properties of individual transistors, no two of which are the same.

Of course, biological retinas have precisely the same problem. No two receptors have the same sensitivity, and no two synapses have the same strength. The problem in wetware is even more acute than it is in silicon. Neural circuitry has *no idea where zero is!* It is also clear that biological systems use adaptive mechanisms to compensate for their lack of precision. The resulting system performance is well beyond that of our most advanced engineering marvels. Once we understand the principles of adaptation, they can be incorporated into a silicon retina.

The most straightforward way to eliminate a fixed-pattern background is to realize that it is not the visual scene itself that carries biologically relevant, real-time information to the brain; it is changes in the scene. The entire visual generation and processing strategy of mammals in general, and humans in particular, is built around sensing changes in retinal input. When a scene is artificially stabilized on the retinal surface, the perception of it fades in a few seconds. When we attempt to stare at a fixed place in a scene, our eyes refuse to do that: they execute microsaccades—tiny, involuntary movements just big enough to generate changes in the receptive circuits. For objects more than a few feet away, our perception of depth is generated when we move our head from side to side to see what moves behind or in front of what else. The bulk of the three-dimensional model our brain makes of our surroundings is generated by a correlation of changes in visual input with our body movements. So the need to work with temporal changes rather than absolute numbers drives the entire organism to adopt strategies for using the most recent changes in sensory input to act upon.

With Misha Mahowald's experience as background, several years of additional biological and engineering analysis, and a more advanced silicon process, Kwabena Boahen had improved the retina model in many ways. The schematic of Kwabena's 1997 adaptive retina pixel is shown in Figure 6:

Kwabena described his improvements as follows (Boahen, 1997):

I describe a retinomorph vision chip that uses neurobiological principles to perform all four major operations found in biological retinae:

1. Continuous sensing for detection;
2. Local automatic gain control for amplification;
3. Spatiotemporal bandpass filtering for preprocessing;
4. Adaptive sampling for quantization.

All four operations are performed right on the focal plane, at the pixel level . . .



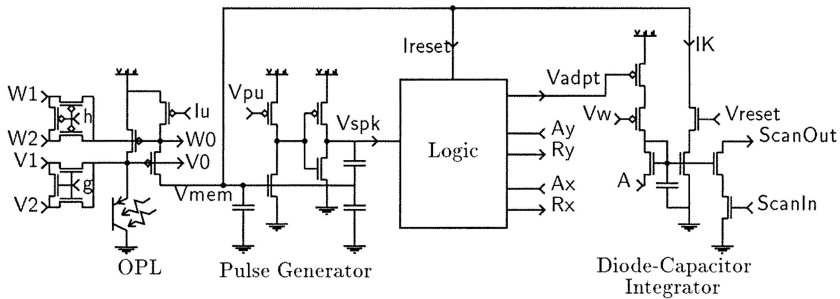


Figure 6: Boahen adaptive pixel schematic.

1. By using local gain control for amplification, I extend the dynamic range without sacrificing sensitivity. Logarithmic compression, in contrast, trades sensitivity for dynamic range;
2. By using a spatiotemporal bandpass for preprocessing, I cut out wideband spatial and temporal noise. Highpass filtering, in contrast, amplifies high-frequency signals with poor signal-to-noise ratios;
3. By using an adaptive neuron for quantization, I increase the sampling rate and reduce the latency—without increasing the average firing rate. A simple integrate-and-fire neuron, in contrast, must maintain a high steady-state firing rate to sample high-frequency signals.

Kwabena's retina also had a scanner for getting ordinary video images, in addition to its independent address-event system for encoding events in the image. Some contemporary cameras have a similar arrangement (Brandli, Berner, Yang, Liu, & Delbruck, 2014).

The analog processing in these early retinas was done without regard to minimizing the number of transistors; the goal was to understand the principles used by biological systems, not to develop commercial products. Of course, economically viable products require exquisite care in the efficient use of silicon area. All of the early retinas were also far more sensitive to transistor variability than could be tolerated in a commercial product. One of the reasons Mach-type center-surround adaptation has not yet been included in commercial event sensors is that all the early designs used a large number of transistors per pixel to realize the resistive network. Recently, Delbruck, Li, Graca, and McReynolds (2022) detailed an adaptive pixel that realizes its resistive network with thin "wires" of polysilicon—a "resistor" layer available in many commercial processes. Many of us had estimated that such an approach would require too much power, but Delbruck et al. (2022) show that it can be done with a few extra milliwatts.

**5.3 Interchip Communication.** Misha Mahowald was keenly aware of the need for compact representation of sensory information, not only from the silicon retina but from neuromorphic chips in general. The following are excerpts from her 1992 thesis (Mahowald, 1992):

Communication between neuronal elements is a principal limiting factor in the design of VLSI neuromorphic systems. This fact is not surprising considering that a large fraction of the volume of the nervous system is composed of myelinated axons. The degree of convergence and divergence of single neurons is staggering in comparison with man-made computers. It might appear impossible, even in principle, to build such structures in VLSI circuits, which are limited to an almost two-dimensional plane of silicon. Surprisingly, the cortices of the brain are nearly two-dimensional as well . . . There is nothing fundamental about the structure of neural tissue that cannot be embedded in silicon. . . . Connections between silicon neurons located on different chips are essential for building even moderately-sized artificial neural systems. . . .

The degree of connectivity and the real-time nature of neural processing demand different approaches to the problem of interchip communication than those used in traditional digital computers. . . . Applications such as sensory transduction, in which the silicon surface acts as a sensory epithelium, require many neurons to be placed on the same chip. The total number of neurons in such a structure greatly exceeds the number of pins available for transmitting their outputs to off-chip targets. The standard approach to resolving this difficulty is to sample and transmit the states of the neurons in sequence. In this case, continuous time communication must be sacrificed in order to time-multiplex the outputs of many neurons onto a small number of wires. The output of each neuron is sampled and transmitted for a brief time. The speed at which data can be transmitted determines the frequency above which information will be lost due to temporal aliasing.

Traditional multiplexing schemes are serial access. Each node is polled in fixed sequence, and its output sent off-chip. Each time slot is allocated to a particular node, and the receiving device must be synchronized with the sending device in order to preserve the identity of the transmitting node. Most multiplexing schemes rely on a global clock to perform this synchronization. Global clock signals may be skewed to the point of dysfunction if the chips comprising the system are too far from each other.

The choice of multiplexing technique depends on how the neural elements in the system encode information. Some systems use analog-valued outputs, which encode several bits of information on a single wire. In analog multiplexed systems, the receiver chip samples the data stream and holds the data in a buffer until the next frame. This approach is particularly useful for interacting with video equipment, as such equipment is designed to work with analog-valued image frames. However, analog data transfer is difficult between chips, in part because the analog data are easily perturbed by noise due to multiplexing. More important, the

variations in the parameters of fabrication on different wafers means that different chips will have disparate interpretations of analog voltages. These difficulties are avoided by transmitting digital amplitude signals.

Both synchronous and asynchronous techniques have been used to time-multiplex digital amplitude data. . . . Digital signal transmission can be very fast because the settling time for an analog amplifier is avoided. Furthermore, digital signals are noise resistant and independent of variations in fabrication parameters. Synchronous transmission of multiple bits of information has the drawback that synchronous switching of many elements causes noise on the power supply.

Asynchronous serial digital communication methods in which the duration of the digital pulse encodes several bits of information have been used. . . . The duration of the pulse is inversely proportional to the analog value of the output. Rather than using a global clocking mechanism to allocate specific time-slots to particular nodes, the identity of the sending neuron is determined by its position in the pulse stream. The node position is computed from the number of transitions in the stream itself. The pulse stream provides its own clock. The pulse stream technique uses time to encode analog state, rather than to communicate explicitly temporal information. . . .

. . . **The Address-Event Representation:** The interchip communication protocol that we have developed is an asynchronous digital multiplexing technique which uses an address-event representation. The address-event representation has much in common with the action-potential representation used by real neurons. Like neuronal action potentials, events in this system are stereotyped digital amplitude events and the interval between events is analog. Information is encoded in the time between events. The principle of this encoding scheme is that  $N$  axonal fibers, with one active at a time, can be replaced by  $(1 + \log N)$  wires, which are simultaneously active. Several fibers in a real nerve bundle may be simultaneously active and so violate the encoding condition. This situation can be dealt with in the address-event representation by making the event duration very short (approximately  $1 \mu\text{second}$ ) compared with the width of neural action potentials (approximately  $0.5 \text{ millisecond}$ ). Short-duration events have small opportunity to overlap. Since, as in a real neuron, the maximum firing rate of a node is limited, even if events from several nodes did occur synchronously, they could be arbitrarily arranged so that they occurred in close succession with little loss of information. . . .

The neurons in the sender array generate a temporal sequence of digital amplitude events to encode their output, a representation conceptually equivalent to a train of action potentials. Each neuron is associated with a digital address which uniquely identifies it. Whenever a neuron signals an event, the multiplexing circuitry broadcasts that neuron's address on the interchip data bus. The nodes have a refractory period that limits the frequency at which they can issue events. The interevent interval at a neuron is much longer than the time required to broadcast the neuron's address. Therefore, many addresses can be multiplexed on the same bus.

The receiver interprets the broadcast of the address as an event that corresponds to the occurrence of an action potential from the neuron identified by that address. For this reason, we have named our communication code an address-event representation.

Misha wrote these cogent comments based on seven years of conceptualizing, designing, constructing, and debugging a complete system in which two silicon retinas communicated critical points of interest in their respective visual fields to a stereo-matching chip, which computed the distance to each point of interest. The realization of this binocular stereopsis function in neuromorphic silicon was a monumental achievement: it set a standard for the entire field, now recognized by the annual Misha Mahowald Prize for Neuromorphic Engineering (<https://www.mahowaldprize.org/home>).

The interchip communication for this remarkable system was done using the address-event protocol. The details of the communication system were developed by a close collaboration of Misha (Mahowald, 1992) and Mass Sivilotti (1991), with coaching from Alain Martin. By the time the system was working, the entire Caltech neuromorphic lab had come to a common understanding, epitomized by Misha (1992):

The relationship between neural systems and VLSI is rooted in the shared limitations imposed by performing computation in similar physical media. The systems discussed in this text support the belief that the physical limitations imposed by the computational medium have as significant an effect on the algorithm. Since circuits are essentially physical structures, I advocate the use of analog VLSI as powerful medium of abstraction, suitable for understanding and expressing the function of real neural systems. The working chip elevates the circuit description to a kind of synthetic formalism. Thus, the physical circuit provides a formal test of theories of function that can be expressed in a circuit language. . . .

Circuit language exists only in embryonic form . . . However, dramatic progress has been made toward standardizing design techniques in the related field of digital VLSI design. There is every reason to believe that similar techniques will emerge in the field of neuromorphic analog design. The address-event communications protocol described in Chapter 2 is a major step towards such a standardization.

Misha's prescient vision—that neuromorphic subsystem developers would develop a common "event" protocol that allows universal interconnection and sparsifies wiring and timing of signal transmission—has come to pass. Even before her original system was fully working, members of the group (Kwabena Boahen, Tobi Delbruck, John Lazzaro, Mass Sivilotti, and John Wawrzynek; Boahen, 2000), working with Alain Martin, were developing more efficient and more robust versions of this important protocol. That effort continues today.

The entire class of dynamic vision sensors (DVS), also called "event cameras" (Gallego et al., 2020), uses some variant of this protocol. Since

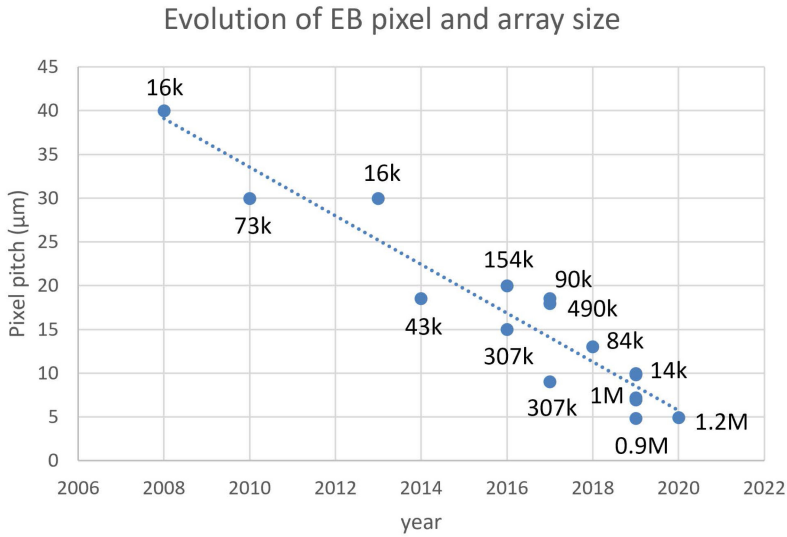


Figure 7: Evolution of the pixel pitch in event vision sensors. (From Posch in Christensen et al., 2022, section 4.4. Used with permission.)

those early days, the capability of event vision sensors has increased along Moore's law, as shown in Figure 7.

Posch, Serrano-Gotarredona, Linares-Barranco, and Delbruck (2014) report the progress:

For over ten years, AER sensory systems were reported by only a handful of research groups (Lazzaro, Wawrzynek, Mahowald, Sivilotti, & Gillespie, 1993; Kumar, Himmelbauer, Cauwenberghs, & Andreou, 1998; Boahen, 1999). However, during these years, some basic progress was made. A better understanding of asynchronous design (Sparso & Furber, 2002; Martin & Nystrom, 2006), leading to robust unarbitrated (Mortara, Vittoz, & Venier, 1995) and arbitrated (Boahen, 2000) asynchronous event read-out, combined with the availability of user-friendly field-programmable gate array (FPGA) external support for interfacing, and new submicrometer technologies allowing complex pixels in reduced areas, heralded a new trend in AER bioinspired spiking sensor developments. Since 2003, many researchers have embraced this trend and AER has been widely used.

Modern event sensors feature stacked pixels, where the processing circuitry is shielded from the optical input by the photodiode. This arrangement enables much better area usage for both light detection and signal processing. (See Lichtsteiner, Posch, & Delbruck, 2008; Suh et al., 2020; Kaas & Hackett, 2000.) Each level can be optimized for its dedicated function. Data

rates of address-event outputs have scaled up remarkably over the past two decades—from approximately 1 MHz to hundreds of MHz or even GHz (Finateu et al., 2020) using a compressed group readout (Son et al., 2017).

For the first time, we have real-time visual event data available from leading-edge, industrial-scale products. Mixed-signal event-based auditory sensors are nearing production phase, and highly efficient digital-signal-processing versions, such as described in Dick Lyon’s book (2017), are mainstream in modern speech-recognition apps and services. Both approaches, or some hybrid approach (Kim et al., 2022), are perfectly good sources of real-world, real-time events. Event-based processing in both visual and auditory domains is essential for systems that must operate in real time in the real world. Compelling examples have been discussed for the visual domain. Events also show great potential for representing the many time-critical aspects of auditory processing, like sound localization, featured in issue 1 of *Neural Computation* (Lazzaro & Mead, 1989; Liu, Strachan, & Basu, 2022).

So now that we have virtually unlimited sources of event signals, how do we process this real-time information with the kind of efficiency displayed by the brain? A good way to start might be to step back and take a more holistic view of the brain.

## 6 Computation with Events

---

Using the auditory system, once again, as our example, let’s take a look at the large-scale organization of the brain, shown in Figure 8.

Colored squares signify physically distinct patches of the cortex, and black lines signify bundles of myelinated nerve fibers. The auditory nerve comes into the pink areas at the bottom of the diagram. Here again, each pulse signals an event, identified by the fiber carrying it and the time of its arrival.

At least 40 years ago, auditory neurobiologists recorded trains of nerve pulses from a whole selection of auditory areas (from the bottom of the diagram to the top), while they were playing music to the animal. On a whim, they decided to listen to the spike trains, which is possible because they are, after all, just waveforms. Starting at the cochlear nucleus, they could hear the spikes, and they could discern the music—loud and clear. As they listened to areas farther and farther up in the diagram, the spike patterns became increasingly noisy due to spikes encoding information at higher levels of representation—but they could still hear the music.

We have discussed at length why it makes sense to encode sensory information by events, but it may come as a surprise that information sent from one area of the brain to another, even very high in the diagram, is encoded the same way. So the entire brain computes with events. We are sensory-dominated creatures. Even our highest thoughts are often “visualized” or “imagined” in sensory terms. It all makes sense.

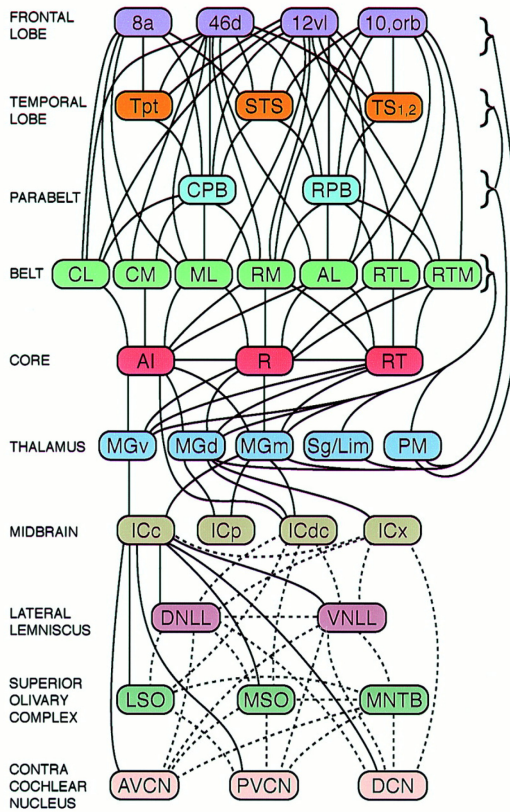


Figure 8: Interconnections between auditory areas in the brain. (Graph: Kaas & Hackett, 2000.)

Computing directly on events has been difficult; our digital technology largely operates on regular “clock” signals that regulate when data are passed from one computing stage to another. Synchronizing events with such a system often compromises the immediate, low-latency advantage of the event representation.

**6.1 Neural Event Coding and Decoding.** The neural code can be thought of in the following terms:

1. Wherever in the brain information is transmitted, it is represented by events.
2. Each event is a volley of individual digital pulses on a bundle of axons.

3. Event identity is encoded in the relative time of arrival of the individual pulses on their specific single nerve fiber of the bundle.
4. Any subset of the individual pulses represents the same event as the entire volley.

Events are decoded in the dendritic trees of receiving neurons. The fiber carrying the first event of the sequence synapses onto the most distal branch of the neuron. A nerve pulse arriving on that fiber creates an excitatory post-synaptic potential (EPSP), which travels down the tree toward the soma (cell body) of the neuron. Fibers carrying later pulses of the event synapse on the tree in such positions that their EPSPs intercept and strengthen the original EPSP as it travels toward the soma. If the composite EPSP is of sufficient amplitude when it reaches the soma, it causes the neuron to fire, thereby creating a full nerve pulse at its output fiber.

It was observed many years ago (Shepherd, 1996) that when individual pulses arrived at a neuron that had been quiescent for some time, the EPSPs from the most distal synapses were larger than those from synapses closer to the soma. This tells us immediately that the dendritic tree itself has gain. The neuron is equipped with an amazing adaptation (gain-control) system, which increases its gain with time when the tree is not experiencing EPSPs, so it perches the neuron at the most sensitive level for detecting incoming event pulses. When no EPSP has traveled down its tree for a long time, a small subset of one or two members of the event sequence may be enough to make a strong EPSP at the soma.

Another level of gain control is operating on the local group of neurons. It turns up the threshold for firing when the average firing rate in the group gets higher. Thus, the strength of EPSP required to make the neuron fire increases when more neurons in the group (including this one) have been firing. The net result is a system that can operate on a few events—we often make decisions in a dark environment based on a few photons hitting our retina. At the opposite extreme, when lots of events are coming in, the gain-control system operates to make each neuron more selective and to keep the outputs from the group from overwhelming subsequent processing areas that receive its outgoing nerve pulses.

The ability of the brain to operate over this incredible range of sensory input is not just a nice-to-have attribute; it is a central part of how it operates. We saw in both the visual and auditory sensors that gain control not only kept the levels in range; it was an essential part of the signal processing. We see that theme played over again here in higher levels of the brain: gain-control is an essential part of the event decoding. The ability of such neurons to detect arbitrary subsets is extraordinary, and it may be a large part of the reason the brain can do so much with such slow, slimy wetware.

**6.2 Can We Build One?** Making an electronic system that operates with events the way the brain does should be possible. Fortunately, the



availability of event-sensor systems gives us data to work with. The topic has become the center of a growing, vibrant research community. It is prominent in the Neuromorphic Roadmap (Christensen et al., 2022). Intel's Loihi (INRC, 2021) system is event based from the hardware up, and we should expect a great deal of good research to emerge from interfacing it to event-sensory systems. Boahen (2022) has a detailed discussion of the advantages of code and processing sparsity, with suggestions for optimizing power and silicon area, and lots of references. Recently, a spiking protocol has been found that is proven equivalent to normal digital backpropagation (Wunderlich & Pehle, 2021). A good overview is given in Roy, Jaiswal, and Panda (2019).

Because modern integrated circuits have communication times that are orders of magnitude faster than neural wetware, an event can carry more information than just the location of the source. Taking advantage of this highly evolved digital resource is a major direction in all event-based sensors and computing systems (Davies et al., 2018; Hoppner et al., 2021).

## 7 Conceptual Model from 1989

---

Since we are celebrating the first issue of *Neural Computation*, I went back through a review paper I was writing at that time (Mead, 1990). Most of it was pathetically out of date, but there was one section that seemed worth remembering. I have included it below.

### 7.1 Adaptation and Learning.

The adaptive retina is a simple example of a general computation paradigm. We can view the function of a particular part of the nervous system as making a prediction about the spatial and temporal properties of the world. In the case of the retina, these predictions are the simple assertions that the image has no second spatial derivative and no first temporal derivative. If the image does not conform to these predictions, the difference between expectation and experience is sent upward to be processed at higher levels.

A block diagram of the essential structure is shown in Figure 9. The computation consists of a prediction of the input and a comparison of that prediction to the actual input. When the model accurately predicts the input, no information is passed to the next level and no correction is made to the model. When the model fails to predict the input, the difference is used to correct the model, and an output is sent to the next level. Random differences will cause a continued small random walk of the model parameters around that required for correct prediction. Systematic differences will cause the model to center itself over the true behavior of the input. Most routine events are filtered out at low level, reserving the capabilities of higher centers for genuinely interesting events.

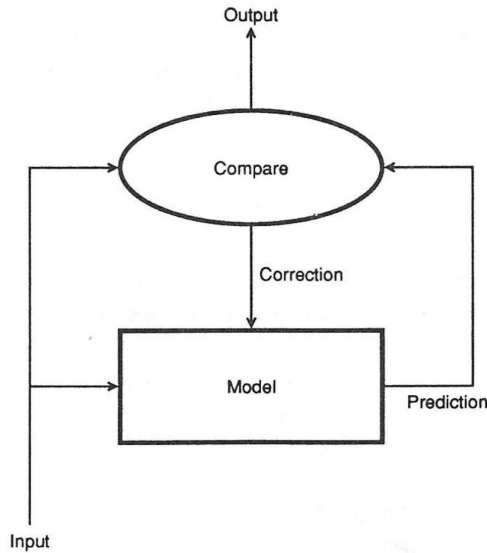


Figure 9: Conceptual arrangement of a single level of a neural processing system.

The box labeled “model” is a predictor, perhaps a crude one; in the case of the retina, the model is the resistive network (Srinivasan, Laughlin, & Dubs, 1982). We give the predictor the input over time, and it computes what is likely to happen next, just before the actual input arrives. When that input materializes, it is compared to the prediction. If the two values are the same, no new information is produced; the system already knew what was about to happen. What happened is what was expected; therefore, no information is sent up to the next level of processing. But when something unexpected has occurred, there is a difference, and that difference is transferred on up to the next level to be interpreted.<sup>3</sup> If we repeat this operation at each level of the nervous system, the information will be of higher quality at each subsequent level because we process only the information that could not be predicted at lower levels. Learning in this kind of system is provided by the adaptation feedback from the comparator to the model. If the model is making predictions that are systematically different from what happens in nature, the ongoing corrections based on the individual differences will cause the model to learn what actually happens, as well as can be captured at its level of representation. It is only those events that are truly random, or that cannot be predicted from this level and therefore appear random, that will cancel out over all experience. The system parameters will undergo a local

<sup>3</sup>This principle has come back in recent time in the form of explicit representation of residuals (He, Zhang, Ren, & Sun, 2016).

random walk but will stay nearly centered on the average of what nature is providing as input. The retina is presented with a wide variety of scenes; it sees white edges and black edges. But every pixel in the retina sees the same intensity, averaged over time. Corrections toward this average constantly correct differences in photoreceptor sensitivity and variation in the properties of individual neurons and synapses. All other information is passed up to higher levels. Even this simple level of prediction removes a great deal of meaningless detail from the image and provides a higher level of representation for the next level of discrimination. That a system composed of many levels organized along the lines of Figure 9 can compute truly awesome results is perhaps not surprising: each level is equipped with a model of the world, as represented by the information passed up from lower levels. All lower-level processing may, from the point of view of a given level, be considered preprocessing. The most important property of this kind of system is that the same mechanism that adapts out errors and mismatches in its individual components also enables the system to build its own models through continued exposure to information coming in from the world. Although this particular example of the adaptive retina learns only a simple model, it illustrates a much more general principle: this kind of system is self-organizing in the most profound sense.

Recently, the deep learning network GPT-3—the one we used as our benchmark network in earlier sections—actually works this way. For each presentation, they show it a couple of pages of text and teach it to predict the next word. After training it using approximately  $5 \times 10^{18}$  floating-point operations, the network displayed remarkable performance on natural-language tasks, for example, generating credible news briefs (Boahen, 2022; Manning, 2022).

This kind of (potentially real-time) training (LeCun & Misra, 2021) is complementary to the standard training when “truthed” data sets are available. It has many advantages in real-world settings, among which are:

1. It does not require “truthed” data sets for training.
2. Training is not a separate process; it is a part of normal operation.
3. Ongoing lifelong learning is a natural aspect of normal operation.

The evolution of microelectronic technology has brought us to the point where we can see a path to realizing systems that sense and process the world around them much the way we humans do. The present digital culture only deals with a highly stylized part of our world. That is why predictions of, for example, ubiquitous autonomous robots have been so wildly overoptimistic.

Networks trained on the digital world are getting good at operating in that world. Fortunately, the digital world is encountering the natural world more and more frequently as we progress. Neuromorphic engineering is bound to contribute to the “naturalization” of the digital world as a normal counterbalance to the ongoing digitization of the natural world. In the

process, we are finding that both natural and manufactured systems are both analog and digital.

## 8 Conclusion

---

I have been privileged to work actively on modern information technology since the year Bob Noyce contributed its enabling invention, the monolithic integrated circuit. The close-up experiences gained over that amazing period have given me a somewhat unique view of the basic nature of the technology evolution process. The individuals whose contributions I have featured in this review each epitomize the impact that a single individual can have by actualizing the right idea at the right time. We are still early in the process of understanding the basic principles of neural computation in a way that they can be actualized. My message to young people in this field is this: You will have inspirations beyond accepted practice and current thought. Be bold: Actualize them. Some could change the world. It will not be easy: You will be treated with skepticism, or outright ignored, but it's worth the struggle.

## Acknowledgments

---

First and foremost, the late Misha Mahowald introduced me to the retina and led me to the neuromorphic way of thinking. Her deep insights and astounding circuit and system creations set the standard to which we all continue to aspire.

The viewpoint expressed in this review is the result of my own work experience and discussions over many years with collaborators, friends, acquaintances, reviewers, and total strangers. To list everyone would take an entire page, and I would still miss many, so I won't even try: you know who you are, and I sincerely thank you! Of decisive help during the preparation of this review were Yaser Abu-Mostafa, Kwabena Boahen, Tobi Delbruck, Shih-Chii Liu, Richard Lyon, and Christoph Posch. Of immense immediate and direct value were extensive critical comments of one anonymous reviewer, including a large number of relevant references of which I was unaware. Responding to these comments has greatly increased the authenticity of the result. Donna Fox introduced me to Overleaf and oversaw the typesetting of the entire document, which included managing all the references and providing instant access to most of them, which makes this review much more useful.

All the above being said, this review contains strong views that are mine alone and should not be blamed on any of the individuals mentioned.

## References

---

- Abu-Mostafa, Y. (1995). Hints. *Neural Computation*, 7(4), 639–671. 10.1162/neco.1995.7.4.639

- Andersch, M., Palmer, G., Krashinsky, R., Stam, N., Mehta, V., Brito, G., & Ramaswamy, S. (2022). *Nvidia Hopper architecture in-depth*. <https://developer.nvidia.com/blog/nvidia-hopper-architecture-in-depth/>
- Boahen, K. (1997). *Retinomorph vision systems: Reverse engineering the vertebrate retina*. Doctoral dissertation, California Institute of Technology. 10.7907/96W6-N605
- Boahen, K. (1999, April). Retinomorph chips that see quadruple images. In *Proceedings of the Seventh International Conference on Microelectronics for Neural, Fuzzy and Bio-Inspired Systems* (pp. 12–20). 10.1109/MN.1999.758840
- Boahen, K. (2000). Point-to-point connectivity between neuromorphic chips using address events. *IEEE Transactions on Circuits and Systems II: Analog and Digital Signal Processing*, 47(5), 416–434. 10.1109/82.842110
- Boahen, K. (2022, February 17). The future of artificial intelligence: 3-D silicon brain. *Chalk Talks series of the Institute for Neural Computation (UC San Diego)*, Stanford, CA. <https://www.youtube.com/watch?v=zWkpVHDmP9s>
- Brandli, C., Berner, R., Yang, M., Liu, S. C., & Delbruck, T. (2014). A  $240 \times 180$  130 dB  $3 \mu\text{s}$  latency global shutter spatiotemporal vision sensor. *IEEE Journal of Solid-State Circuits*, 49(10), 2333–2341. 10.1109/JSSC.2014.2342715
- Cerebras (2022). Retrieved 2022. <https://cerebras.net/>
- Christensen, D., Dittmann, R., Linares-Barranco, B., Sebastian, A., Le Gallo, M., Redaelli, A., . . . Pryds, N. (2022). 2022 roadmap on neuromorphic computing and engineering. *Neuromorphic Computing and Engineering*, 2, 022501. 10.1088/2634-4386/ac4a83
- Dally, W. Gray, C., Poulton, J., Khailany, B., Wilson, J., & Dennison, L. (2018). Hardware-enabled artificial intelligence. In *Proceedings of the 2018 IEEE Symposium on VLSI Circuits* (pp. 3–6). 10.1109/VLSIC.2018.8502368
- Davies, M., Srinivasa, N., Lin, T., Chinya, G., Cao, Y., Choday, S., . . . Wang, H. (2018). Loihi: A neuromorphic many-core processor with on-chip learning. *IEEE Micro*, 38(1), 82–99. 10.1109/MM.2018.112130359
- Delbruck, T., Li, C., Graca, R., & Mcreynolds, B. (2022). *Utility and feasibility of a center surround event camera*. arXiv:2202.13076.
- Delbruck, T., & Liu, S.-C. (2019). Data-driven neuromorphic DRAM-based CNN and RNN accelerators. In *Proceedings of the 53rd Asilomar Conference on Signals, Systems, and Computers* (pp. 500–506). 10.1109/IEEECONF44664.2019.9048865
- Diorio, C., Hasler, P., Minch, B., & Mead, C. (1996). A single-transistor silicon synapse. *IEEE Transactions on Electron Devices*, 43(11), 1972–1980. 10.1109/16.543035
- Durbin, R., & Rumelhart, D. (1989). Product units: A computationally powerful and biologically plausible extension to backpropagation networks. *Neural Computation*, 1(1), 133–142. 10.1162/neco.1989.1.1.133
- Finateu, T., Niwa, A., Matolin, D., Tsuchimoto, K., Mascheroni, A., Reynaud, E., . . . Posch, C. (2020). 5.10 A  $1280 \times 720$  back-illuminated stacked temporal contrast event-based vision sensor with  $4.86 \mu\text{m}$  pixels, 1.066 GEPS readout, programmable event-rate controller and compressive data-formatting pipeline. In *Proceedings of the 2020 IEEE International Solid-State Circuits Conference* (pp. 112–114). 10.1109/ISSCC19947.2020.9063149

- Gallego, G., Delbruck, T., Orchard, G., Bartolozzi, C., Taba, B., Censi, A., . . . Scaramuzza, D. (2020). Event-based vision: A survey. *IEEE Transactions on Pattern Analysis and Machine Intelligence*, 44(1), 154–180. 10.1109/TPAMI.2020.3008413
- Goda, A. (2020). 3-D NAND technology achievements and future scaling perspectives. *IEEE Transactions on Electron Devices*, 67(4), 1373–1381. 10.1109/TED.2020.2968079
- Gollisch, T., & Meister, M. (2008). Rapid neural coding in the retina with relative spike latencies. *Science*, 319(5866), 1108–1111. 10.1126/science.1149639
- He, K., Zhang, X., Ren, S., & Sun, J. (2016). Deep residual learning for image recognition. In *Proceedings of the 2016 IEEE Conference on Computer Vision and Pattern Recognition* (pp. 770–778). 10.48550/ARXIV.1512.03385
- Hinton, G. E., Krizhevsky, A., & Wang, S. D. (2011, June). Transforming auto-encoders. In *Proceedings of the International Conference on Artificial Neural Networks* (pp. 44–51). Springer.
- Hinton, G., Srivastava, N., Krizhevsky, A., Sutskever, I., & Salakhutdinov, R. (2012). *Improving neural networks by preventing co-adaptation of feature detectors*. arXiv:1207.0580.
- Hoppner, S., Yan, Y., Dixius, A., Scholze, S., Partzsch, J., Stolba, M., . . . Mayr, C. (2021). *The SpiNNaker 2 processing element architecture for hybrid digital neuromorphic computing*. arXiv:2103.08392.
- Intel Neuromorphic Research Community (INRC). (2021). *Partner quotes in support of Loihi 2 launch*. <https://download.intel.com/newsroom/2021/new-technologies/intel-labs-loihi-2-lava-quotes.pdf>
- IEEE International Conference on Solid-State Circuits (ISSCC). (2022). In *Proceedings of the 2022 IEEE International Solid-State Circuits Conference*. 10.1109/ISSCC42614.2022
- Jouppi, N., Young, C., Patil, N., Patterson, D., Agrawal, G., Bajwa, R., . . . Yoon, D. (2017). In-datacenter performance analysis of a tensor processing unit. In *Proceedings of the 44th Annual International Symposium on Computer Architecture* (pp. 1–12). 10.1145/3079856.3080246
- Kaas, J., & Hackett, T. (2000). Subdivisions of auditory cortex and processing streams in primates. In *Proceedings of the National Academy of Sciences*, 97(22), 11793–11799. 10.1073/pnas.97.22.11793
- Kim, K., Gao, C., Graça, R., Kiselev, I., Yoo, H.-J., Delbruck, T., & Liu, S.-C. (2022). A 23  $\mu$ W solar-powered keyword-spotting ASIC with ring-oscillator-based time-domain feature extraction. In *Proceedings of the 2022 IEEE International Solid-State Circuits Conference* (pp. 1–3). 10.1109/ISSCC42614.2022.9731708
- Kim, K., & Liu, S.-C. (2022). *Continuous-time analog filters for audio edge intelligence: Review and analysis on design techniques*. arXiv:2206.02639.
- Krizhevsky, A. (2021). *Alex Krizhevsky*. [https://en.wikipedia.org/wiki/Alex\\_Krizhevsky](https://en.wikipedia.org/wiki/Alex_Krizhevsky)
- Krizhevsky, A., & Hinton, G. (2009). *Learning multiple layers of features from tiny images*. 10.1.1.222.9220
- Krizhevsky, A., & Hinton, G. (2010). *Convolutional deep belief networks on CIFAR-10*. Unpublished manuscript. <https://www.cs.toronto.edu/kriz/conv-cifar10-aug2010.pdf>

- Krizhevsky, A., Sutskever, I., & Hinton, G. (2017). ImageNet classification with deep convolutional neural networks. *Communications of the ACM*, 60(6), 84–90. 10.1145/3065386
- Kumar, N., Himmelbauer, W., Cauwenberghs, G., & Andreou, A. (1998). An analog VLSI chip with asynchronous interface for auditory feature extraction. *IEEE Transactions on Circuits and Systems II: Analog and Digital Signal Processing*, 45(5), 600–606. 10.1109/82.673642
- Kung, H. (1979). Let's design algorithms for VLSI systems. In *Proceedings of the Caltech Conference on Very Large Scale Integration*, California Institute of Technology (pp. 65–90). <https://caltechconf.library.caltech.edu/192/1/HTKung.pdf>
- Kung, H. (1982). Why systolic architectures? *Computer*, 15(1), 37–46. 10.1109/MC.1982.1653825
- Kung, H. & Leiserson, C. (1979). Systolic arrays (for VLSI). In *Sparse Matrix Proceedings*, 1, 256–282.
- Lardinois, F. (2013). *How Google's acquisition of DNNresearch allowed it to build its impressive Google+ photo search in 6 months*. techcrunch.com. <http://tcrn.ch/11zxcga>
- Lazzaro, J., & Mead, C. (1989). A silicon model of auditory localization. *Neural Computation*, 1(1), 47–57. 10.1162/neco.1989
- Lazzaro, J., Wawrzynek, J., Mahowald, M., Sivilotti, M., & Gillespie, D. (1993). Silicon auditory processors as computer peripherals. *IEEE Trans. Neural Networks*, 4(3), 523–528. 10.1109/72.217193
- LeCun, Y., & Misra, I. (2021). *Self-supervised learning: The dark matter of intelligence*, 2021. <https://ai.facebook.com/blog/self-supervised-learning-the-dark-matter-of-intelligence>
- Lichtsteiner, P., Posch, C., & Delbruck, T. (2008). A 128 × 128 120 dB 15 μs latency asynchronous temporal contrast vision sensor. *IEEE Journal of Solid-State Circuits*, 43(2), 566–576. 10.1109/JSSC.2007.914337
- Lippmann, R. (1989). Review of neural networks for speech recognition. *Neural Computation*, 1(1), 1–38. 10.1162/neco.1989.1.1.1
- Liu, S.-C. (2022). Section number: Neuromorphic audition. In *Roadmap on neuromorphic computing and engineering* (pp. 142–145). IOP Publishing. 10.1088/2634-4386/ac4a83
- Liu, S.-C., Strachan, J., & Basu, A. (2022). Prospects for analog circuits in deep networks. In P. Harpe, K. A. A. Makinwa, & A. Baschiroto (Eds.), *Analog circuits for machine learning: Current/voltage/temperature sensors, and high-speed communication* (pp. 49–61). Springer.
- Lyon, R. (2017). *Human and machine hearing: Extracting meaning from sound*. Cambridge University Press. 10.1017/9781139051699
- Mahowald, M. (1992). *VLSI analogs of neuronal visual processing: A synthesis of form and function*. Doctoral dissertation, California Institute of Technology. 10.7907/4bdw-fg34
- Mahowald, M., & Mead, C. (1988). A silicon model of early visual processing. *Neural Networks*, 1, 91–97. 10.1016/0893-6080(88)90024-X
- Manning, C. (2022). Human language understanding and reasoning. *Daedalus*, 151(2), 127–138. <https://direct.mit.edu/daed/article/151/2/127/110621/Human-Language-Understanding-amp-Reasoning>. 10.1162/daed\_a\_01905

- Martin, A., & Nystrom, M. (2006). Asynchronous techniques for system-on-chip design. In *Proceedings of the IEEE*, 94(6), 1089–1120. 10.1109/JPROC.2006.875789
- Mead, C. (1990). Neuromorphic electronic systems. In *Proceedings of the IEEE*, 78(10), 1629–1636. 10.1109/5.58356
- Mead, C., & Mahowald, M. (1984). *An electronic model of the Y-system of mammalian retina*. Internal Technical Memo 5144: DF: 84. California Institute of Technology. <https://resolver.caltech.edu/CaltechAUTHORS:20220523-171311035>
- Mortara, A., Vittoz, E., & Venier, P. (1995). A communication scheme for analog VLSI perceptive systems. *IEEE Journal of Solid-State Circuits*, 30(6), 660–669. 10.1109/4.387069
- Mythic-ai.com (2021). *M1076 Analog Matrix Processor—Mythic*. <https://www.mythicalai.com/product/m1076-analog-matrix-processor/>
- Nair, V., & Hinton, G. (2010). Rectified linear units improve restricted Boltzmann machines. In *Proceedings of the 27th International Conference on Machine Learning* (pp. 807–814). <https://icml.cc/Conferences/2010/papers/432.pdf>
- Parisi, G., Kemker, R., Part, J., Kanan, C., & Wermter, S. (2019). Continual lifelong learning with neural networks: A review. *Neural Networks*, 113, 54–71. 10.1016/j.neunet.2019.01.012
- Posch, C., Serrano-Gotarredona, T., Linares-Barranco, B., & Delbruck, T. (2014). Retinomorphomorphic event-based vision sensors: Bioinspired cameras with spiking output. In *Proceedings of the IEEE*, 102(10), 1470–1484. 10.1109/JPROC.2014.2346153
- Ratliff, F. (1965). *Mach bands: Quantitative studies on neural net-works in the retina* (pp. 253–332). Holden-Day. <https://books.google.com/books?id=iwwpAQAAMAAJ>
- Redmond, K., & Smith, T. (1980). *Project Whirlwind: The history of a pioneer computer*. Digital Press. <https://books.google.com/books?id=CmBTAAMAAAJ&q=1947>
- Roy, K., Jaiswal, A., & Panda, P. (2019). Towards spike-based machine intelligence with neuromorphic computing. *Nature*, 575(7784), 607–617. 10.1038/s41586-019-1677-2
- Rumelhart, D., Hinton, G., & Williams, R. (1986). Learning internal representations by error propagation. In D. E. Rumelhart, J. L. McClelland, and the PDP Research Group, *Parallel distributed processing* (pp. 318–362). MIT Press.
- Sarpeshkar, R. (2010). *Ultra low power bioelectronics: Fundamentals, biomedical applications, and bio-inspired systems*. Cambridge University Press. 10.1017/CBO9780511841446
- Saunders, W. (2012). *Visualizing trends in “energy per operation.”* Datacenter Knowledge. <https://www.datacenterknowledge.com/archives/2012/12/06/visualizing-trends-in-energy-per-operation>
- Schlottmann, C., & Hasler, P. (2011). A highly dense, low power, programmable analog vector-matrix multiplier: The FPAA implementation. *IEEE Journal on Emerging and Selected Topics in Circuits and Systems*, 1(3), 403–411. 10.1109/JETCAS.2011.2165755
- Sebastian, A., Le Gallo, M., Khaddam-Aljameh, R., & Eleftheriou, E. (2020). Memory devices and applications for in-memory computing. *Nature Nanotechnology*, 15(7), 529–544. 10.1038/s41565-020-0655-z



- Shepherd, G. (1996). The dendritic spine: A multifunctional integrative unit. *Journal of Neurophysiology*, 75(6), 2197–2210. 10.1152/jn.1996.75.6.2197
- Sivilotti, M. (1991). *Wiring considerations in analog VLSI systems, with application to field-programmable networks*. Doctoral dissertation, California Institute of Technology. 10.7907/stj4-kh72
- Sommer, J., Özkan, M., Keszocze, O., & Teich, J. (2022). *Efficient hardware acceleration of sparsely active convolutional spiking neural networks*. arXiv:2203.12437[Cs].
- Son, B., Suh, Y., Kim, S., Jung, H., Kim, J.-S., Shin, C., . . . Ryu, H. (2017). 4.1A 640 × 480 dynamic vision sensor with a 9 μm pixel and 300Meps address-event representation. In *Proceedings of the 2017 IEEE International Solid-State Circuits Conference* (pp. 66–67). 10.1109/ISSCC.2017.7870263
- Sparso, J., & Furber, S. (2002). *Principles of asynchronous circuit design*. Springer.
- Srinivasan, M., Laughlin, S., & Dubs, A. (1982). Predictive coding: A fresh view of inhibition in the retina. In *Proc. R. Soc. Lond.: B Biol. Sci.*, 216, 427–459. 10.1098/rspb.1982.0085
- Suh, Y., Choi, S., Ito, M., Kim, J., Lee, Y., Seo, J., . . . Park, Y. (2020). A 1280 × 960 dynamic vision sensor with a 4.95-μm pixel pitch and motion artifact minimization. In *Proceedings of the 2020 IEEE International Symposium on Circuits and Systems* (pp. 1–5). 10.1109/ISCAS45731.2020.9180436
- Watts, L., & Mead, C. (1993). *Cochlear mechanics: Analysis and analog VLSI*. Doctoral dissertation, California Institute of Technology. 10.7907/19EW-YM12
- Wunderlich, T., & Pehle, C. (2021). Event-based backpropagation can compute exact gradients for spiking neural networks. *Scientific Reports*, 11(1), 1–17. 10.1038/s41598-021-91786-z

---

Received February 22, 2022; accepted August 21, 2022.